L-statistics based Space/Spatial-Frequency Filtering of 2D signals in heavy tailed noise

Irena Orović and Srdjan Stanković

Abstract—Most of the commonly used stationary filtering techniques, performed either in the spatial or frequency domains, fail to produce good results for noisy signals with fast varying non-stationary structures. The filtering results could be improved by using space/spatial-frequency based non-stationary filters. Hence, a robust approach to space/spatial-frequency analysis of two-dimensional noisy signals is proposed in this paper. It is based on the two-dimensional L-estimate forms of the short-time Fourier transform, the spectrogram and the S-method. The proposed space/spatial-frequency distributions are used to define the L-estimate space-varying filtering procedure. It is designed for denoising of 2D non-stationary signals affected by the strong impulsive or mixed heavy-tailed and Gaussian noise. The efficiency of the proposed procedure is tested on the examples with interferogram-like images, textures and satellite images.

***Index Terms*— robust estimators, space/spatial-frequency distribution, L-estimate forms, robust space-varying filtering**

1. INTRODUCTION

In many real applications signals are often corrupted by noise. Depending on its statistics, noise is usually Gaussian, impulse, mixed Gaussian and impulse noise, or some other heavy-tailed noise (such as Cauchy or α-stable noise) [1]. The second classification is based on spectral density which can be used to distinguish between coloured (correlated) and white (uncorrelated) noise. Noise is present in images as film grain, photoelectronic or salt and pepper noise, which can be caused by transmission errors, faulty memory locations, etc. Linear filters fail to effectively remove heavy-tailed noise and they usually produce blurred representation with destroyed lines and fine details [2], [3]. The non-linear filters [3]-[6], such as different variations of median based filters, attempt to resolve this issue, but it is still difficult to preserve the finer structures especially for the fast varying details.

This work is supported by the Ministry of Education and Science of Montenegro. Authors are with the Faculty of Electrical Engineering, University of Montenegro, 81000 Podgorica, Montenegro. S. Stanković is on leave at the University of Villanova, Villanova, PA, USA. The corresponding author is Irena Orovic, phone: +382 67 516 795, fax: +382 20 242 667, Email: irenao@ac.me

The methods based on edge-preserving regularization functionals are used to deal with images corrupted by noise. For instance, the total variation method [7] (proposed by Rudin, Oshera and Fatemi - ROF) is based on an L2-norm data fitting term, which means, from a statistical point of view, that it is adapted to deal with Gaussian noise. Hence, these methods fail in the presence of impulse noise, since the restoration would alter considerable amount of pixels in the image, including the non-noisy pixels. Furthermore, the ROF removes the oscillating functions and keeps the part of image formed by homogeneous regions and sharp edges [8]. Therefore, the ROF method removes textures that, just like the noise, represent the oscillating patterns, and thus it is not suitable for filtering of texture-like images. In order to provide better filtering results in the presence of impulse noise, non-smooth data-fidelity terms such (e.g. L1 term) are used together with edge-preserving regularization terms [9],[10]. Most of these filtering techniques are performed either in the spatial or in the frequency domain. However, the joint space/spatial-frequency (SSF) domain should be used for signals that exhibit highly non-stationary characteristics [11]-[16]. Thus, an efficient filtering approach can be obtained by using the concept of space-varying filtering based on the space/spatial-frequency representation [16]. However, the standard SSF representations produce poor results in the presence of heavy-tailed noise. Hence, we need a filter formulation based on the SSF distribution robust to mixed heavy-tailed and Gaussian noise, such as the L-estimate forms [17], [18].

This paper provides an extension of one-dimensional L-estimate robust approach [17] to the SSF representation for analysis of highly non-stationary 2D signals. A basic idea for this approach has been introduced in [19]. Starting from a general signal processing approach based on the robust statistics, the proposed method introduces the 2D form of SSF based non-stationary filtering for signals in impulsive or mixed heavy-tailed and Gaussian noise. The 2D L-estimate forms of the short time-Fourier transform (STFT), the spectrogram and the S-method are introduced. The proposed method is suitable for different types of 2D signals that contain fast-varying details and structures. As particular 2D signal cases that often appear in real applications, we focus on interferograms, textures and surface images. They are characterized by a specific set of frequency components which brings most of the texture elements and details in the spatial domain. In this case, the proposed L-estimate space/spatial-frequency approach can be used to identify important components and isolate them from the scattered noise. However, we should emphasize that the realization and application of SSF analysis for 2D signals are not a straightforward extension of the one-dimensional approach. Namely, the realization depends on the type of noise, but also on the type of 2D signal (e.g., texture, interferogram, satellite image, etc). For instance, the results have shown that the signals characterized by highly enhanced frequency peaks

(interferogram-like signals) can be successfully treated by the L-estimate quadratic distributions, while the L-estimate spectrogram can be used for textures. Also, the window width used in the realization of SSF distribution might influence the performance of the proposed filtering approach. The achieved filtering results are compared through the examples with numerous existing filter forms.

The paper is organized as follows. The L-estimate 2D STFT and the L-estimate 2D S-method are proposed in Section 2. The L-estimate space-varying filtering approach is proposed in Section 3. The experimental results are presented in Section 4, while the concluding remarks are given in Section 5.

2. TWO-DIMENSIONAL ROBUST SPACE/SPATIAL-FREQUENCY DISTRIBUTION FORMS

The maximum likelihood (ML) estimators have been used to design the best estimates for a given distribution of observation errors. Generally, the standard STFT can be obtained as an ML estimate of clean signal in Gaussian noise environment [17]. Thus, the STFT can be obtained as a solution of minimization problem with the loss function equal to the square error. In the case of Laplacian (impulse) noise, the robust distributions have been introduced for loss function equal to the absolute error. However, for the mixture of Gaussian and impulse noise, the probability density function produces a complex form of loss function that is not suitable for minimization [17]. Also, the ML estimates are sensitive to any deviation from the hypothetical distribution. When the resulting signal is a sum of Gaussian and impulse noise, we can calculate the ML estimate of a discrete unitary transform by solving a certain minimization problem based on an appropriate loss function. However, since the resulting loss function has a form that cannot be used practically, Huber's estimation theory [20] provides solutions based on the L and R-estimation approaches. The robust estimators can be efficient for a wide class of the error distributions. Robust means that it is less sensitive to the unknown error distribution (noise pdf), i.e., robustness with respect to model uncertainties. Unlike the estimators that are designed for a nominal model and deteriorate considerably if the actual error model deviates from the one assumed, in the case of robust estimators small deviations from the assumed model should impair the performance only slightly [20], [21].

The L-estimation filters (L-filters) and general Huber estimation theory have attracted significant attention in the signal and image filtering, although most of the solutions provide only the low-pass characteristics [22]-[26]. Namely, to be able to deal with impulsive and nonimpulsive noise components, the L-estimators are linear combinations of order statistics [17],[20],[27]. In other words, the idea behind the L-estimation approach is that the small errors, that are most likely to be Gaussian in origin, are weighted quadratically, while large errors, more likely to be outliers, are weighted heavily. For

non-stationary signals, the solutions based on the L-estimate STFT have been proposed [17]. These results are used here for a definition of the L-estimation SSF forms of the discrete unitary transforms, which produce efficient results for a wide range of weights in the mixed noise.

In the analysis of 2D signals corrupted by the noise, the SSF distributions have been used. The standard SSF distributions provide good performance in the presence of Gaussian noise. However, they produce poor results if noise is heavy-tailed. Hence, in this Section, the two-dimensional robust SSF distributions for analysis of 2D signals in heavy-tailed or mixed noise have been proposed. Later, they will be used to design an efficient robust space-varying filtering procedure.

2.1. Robust form of 2D STFT

Let us consider a 2D noisy signal:

$$f(x,y)=s(x,y)+\nu(x,y), \tag{1}$$

where $s(x,y)$ is a complex-valued signal corrupted by complex-valued noise $v(x,y)$. The general form of the STFT has been defined as a solution of the optimization problem [18], which can be extended to the 2D signal $f(x,y)$ as follows:

$$STFT(x,y,k_x,k_y)=\arg\min_m J(x,y,k_x,k_y,m). \tag{2}$$

The penalty function has been defined as:

$$J(x,y,k_x,k_y,m)=\sum_{u=-N/2}^{N/2-1}\sum_{v=-N/2}^{N/2-1} w_h(u,v)F(\varepsilon(x,y,k_x,k_y,m)), \tag{3}$$

where w_h is the window function (the rectangular window is usually assumed and thus it will be omitted in the sequel), the number of samples within the window is N, while:

$$\varepsilon(x,y,k_x,k_y,m)=f(x+u,y+v)e^{-j2\pi uk_x/N}e^{-j2\pi vk_y/N}-m\,.$$

The function F is called the loss function and its argument is an error function denoted by ε. The error function ε expresses the "similarity" between the signal and a given harmonic $e^{-j2\pi uk_x/N}e^{-j2\pi vk_y/N}$ [18]-[20]. The parameter m within the error function is a desired solution of the imposed optimization problem, which should provide the minimal error. It is a complex-valued optimization parameter which is an estimate of the expectation of the sample average of the quantity $f(x+u,y+v)e^{-j2\pi uk_x/N}e^{-j2\pi vk_y/N}$, [18],[20]. From (2) we might observe that different forms of STFT are obtained as a result of minimizing different forms of F (by equalizing its first derivative to zero), which depends on the

noise statistics [20]. Assuming that the noise probability density function is p_υ, ML estimation is obtained by using the loss function:

$$F(\varepsilon) = -\ln p_\upsilon(\varepsilon). \tag{4}$$

Some special cases, such as Gaussian white noise and impulse noise will be discussed later in this Section. Having in mind that the noise is equally distributed along the axes (x and y axis) and the same loss function F is used, we can calculate the 2D STFT as a composition of 1D cases:

$$\begin{aligned} STFT^{1D}(x,y,k_y) &= \arg\min_m \sum_{v=-N/2}^{N/2-1} F(f(x,y+v)e^{-j2\pi vk_y/N} - m) \\ STFT(x,y,k_x,k_y) &= \arg\min_m \sum_{u=-N/2}^{N/2-1} F(STFT^{1D}(x+u,y,k_y)e^{-j2\pi uk_x/N} - m) \end{aligned} \tag{5}$$

This results in a computationally more efficient method, as it will be discussed in Section 2.2 for a specific case of STFT. It means that the space-varying filtering within the 2D window can be done consecutively along the rows and along the columns, where the separable window function is used.

According to (4), for Gaussian white noise, the loss function will be $F(\varepsilon) = |\varepsilon|^2$. Then, the optimum solution $\hat{m}$, obtained by solving [18]:

$$\frac{\partial J(x,y,k_x,k_y,m)}{\partial m^*}\Big|_{m=m_0} = 0, \; with \; STFT(x,y,k_x,k_y) = m_0 \quad i.e., \tag{6}$$

$$\frac{\sum_{u=-N/2}^{N/2-1}\sum_{v=-N/2}^{N/2-1} \partial\left(\left(f(x+u,y+v)e^{-j2\pi uk_x/N}e^{-j2\pi vk_y/N} - m\right)^2\right)}{\partial m^*} = 0,$$

yields the well-known standard STFT for 2D signals [11]:

$$STFT_S(x,y,k_x,k_y) = STFT(x,y,k_x,k_y) = \sum_{u=-N/2}^{N/2-1}\sum_{v=-N/2}^{N/2-1} f(x+u,y+v)e^{-j2\pi/N(uk_x+vk_y)}. \tag{7}$$

Hence, the standard STFT is a special case of (2), which produces poor results for the impulse noise. In this case, robust estimates are obtained by using the loss function $F(\varepsilon) = |\varepsilon|$ leading to median forms of STFT. For complex valued signals, the robust estimate of the STFT can be obtained by using: vector median approach, where (Re{STFT}, IM{STFT}) are considered as a vector, whose components are mutually independent. We can also use a marginal median approach which treats real and imaginary parts separately, providing a simpler solution: $F(\varepsilon) = |\mathrm{Re}(\varepsilon)| + |\mathrm{Im}(\varepsilon)|$. This function can be combined with the concept of L-estimation. Unlike the median form which uses one central value in the sorted sequence,

the L-estimate approach takes a set of values around the median and calculates their mean. Hence, it discards only the values at the ends of the sorted sequence assuming that they are affected by the noise. Following the concepts introduced for one-dimensional signals [17], the 2D L-estimate robust STFT can be defined as:

$$STFT_L(x,y,k_x,k_y)=\sum_{p=0}^{N-1}\sum_{q=0}^{N-1}a_p a_q(r_{p,q}(x,y,k_x,k_y)+j\cdot i_{p,q}(x,y,k_x,k_y)), \tag{8}$$

where,

$$\begin{aligned} r_{p,q}(x,y,k_x,k_y)&\in\{\mathrm{Re}(f_{x,y,u,v}),\ \ u,v\in[-N/2,N/2)\},\\ i_{p.q}(x,y,k_x,k_y)&\in\{\mathrm{Im}(f_{x,y,u,v}),\ \ u,v\in[-N/2,N/2)\}, \end{aligned} \tag{9}$$

and

$$f_{x,y,u,v}=f(x+u,y+v)e^{-j2\pi(uk_x+vk_y)/N}. \tag{10}$$

The elements: $r_{p,q}$ and $i_{p,q}$ are sorted in non-decreasing order. After the sorting operation, the coefficients corrupted by noisy pulses will be located at the ends of the sorted sequence. Thus, these coefficients should be set to zero, and the mean value is calculated using the remaining ones.

In order to remove impulses and to preserve good resolution, the weights a_p and a_q are designed in analogy with coefficients of α-trimmed filter [17]:

$$a_p=a_q=\begin{cases}\dfrac{1}{N(1-2\alpha)+4\alpha}, & \text{for}\quad p,q\in[(N-2)\alpha,\alpha(2-N)+N-1]\\ 0, & \text{elsewhere,}\end{cases} \tag{11}$$

where N is even, while the parameter α takes values within the range [0,1/2]. Higher α provides better reduction of noise, while smaller α improves spectral characteristics. Thus, the value of parameter α should be carefully chosen. As a special cases, for α=0 and α=1/2, the standard form (given by (7)) and median form of the STFT follow, respectively. Generally, a_p and a_q do not have to be equal, and their values depends on the number of coefficients affected by the impulse noise along x and y coordinate, respectively. Assuming that the noise is distributed equally along both coordinates, we can use a_p=a_q. It is important to note that the value of parameter α should be chosen according to the expected percentage of noisy pulses.

2.2. Realization of the L-estimate 2D STFT

The realization of the 2D $STFT_L$ given by (8) (which is a special case of (2)) requires complex and computationally demanding procedure, with higher processing time and significant hardware resources due to matrix operations. However, an appropriate and simple solution can be obtained by decomposing 2D $STFT_L$ into two sequential 1D $STFT_L$. Firstly, the 1D L-estimate STFT is calculated for each row of the windowed signal as follows:

$$STFT_L^{1D}(x,y,k_x) = \sum_{p=0}^{N-1} a_p (r_p(x,y,k_x) + j \cdot i_p(x,y,k_x)), \tag{12}$$

where $r_p(x,y,k_x)$ and $i_p(x,y,k_x)$ are sorted elements of the following sets:

$$r_u(x,y,k_x) \in \left\{ \mathrm{Re}(f(x+u,y) e^{-j2\pi u k_x / N}) \right\},$$
$$i_u(x,y,k_x) \in \left\{ \mathrm{Im}(f(x+u,y) e^{-j2\pi u k_x / N}) \right\}.$$

Note that 1D STFT is calculated only for one frequency coordinate k_x, and thus, k_y coordinate does not appears in (12).

The calculation is performed through the following steps:

1. Each row of the $f(x,y)$ is multiplied by $e^{-j2\pi u k_x / N}$, for $u \in [-N/2, N/2)$
2. The products are sorted in a non-decreasing order
3. The sorted elements are multiplied by the weights a_p
4. The sum of weighted elements is calculated.

In order to obtain 2D L-estimate STFT, the same procedure is applied to the columns of 1D L-estimate STFT. The result is the 2D L-estimate STFT:

$$STFT_L(x,y,k_x,k_y) = \sum_{q=0}^{N-1} a_q (r_q(x,y,k_x,k_y) + j \cdot i_q(x,y,k_x,k_y)), \tag{13}$$

where r_q and i_q are sorted real and imaginary part of $STFT_L^{1D}(x,y+v,k_x) e^{-j2\pi v k_y / N}$, respectively.

The average processing time in Matlab for window size 64x64 is approximately 0.09 s/pixel (Processor: Intel(R), Core 2 Duo, 2 GHz), while for the window size 9×9, it is approximately 0,0015 s/pixel. Although the software simulation could require significant processing time, an efficient hardware implementation as in [30] can solve this problem. This hardware performs $STFT_L$ for one-dimensional signal. The $STFT_L$ is computationally the most demanding, while the remaining operations in the proposed system have negligible processing time comparing to $STFT_L$. The processing time of

this hardware for a vector with 64 elements in the window is 140ns. If we use the same hardware solution in parallel for 64 rows within the 2D window, while the rest of the processing is done in serial realization, the total processing time would be: $140\text{ns}\cdot 2\cdot 2=560\,\text{ns/pixel}$ (we multiply by 2 because the rows are columns are processed within two passes, and again by 2 because real and imaginary parts are treated separately). The total processing time for an 256×256 image is 36.5 ms. Note that we consider the simplest solution without any optimization regarding computational complexity.

2.3. 2D L-estimate S-method

Generally, the spectrogram is defined as a square module of the STFT. As a special case, the standard spectrogram is obtained using $STFT_S$ given by (7). Similarly, based on the L-estimate STFT, the 2D L-estimate spectrogram follows as:

$$SPEC_L(x,y,k_x,k_y)=\left|STFT_L(x,y,k_x,k_y)\right|^2. \tag{14}$$

The L-estimate spectrogram has a low time-frequency resolution, as it is the case with the standard one. Thus, in order to improve the concentration, the quadratic distributions have been considered. For instance, the S-method has been used in many practical applications [11], [31], [33]. It allows numerically efficient realization, provides good concentration of the signal-components as in the Wigner distribution, and reduces the cross-terms for multicomponent signals. Also, the performances in the noisy environment are improved in comparison with the spectrogram and the Wigner distribution. Here, in order to improve the representation in the presence of heavy-tailed noise, the 2D L-estimate S-method is defined as:

$$SM_L(x,y,k_x,k_y)=\sum_{q_x=-Q}^{Q}\sum_{q_y=-Q}^{Q}STFT_L(x,y,k_x+q_x,k_y+q_y)STFT_L^*(x,y,k_x-q_x,k_y-q_y) \tag{15}$$

The L-estimate S-method (SM_L) is defined as the convolution of $STFT_L$ terms within the 2D frequency domain window (window size is defined by the parameter Q). The convolution should be performed only within the same signal-term (auto-term), avoiding different signal components being convolved. In this case, the S-method improves the concentration of signal components and consequently increases their energy with respect to the noise level. Note that the window has to be narrower than the minimal distance between the auto-terms, because the interactions between auto-terms will produce cross-terms. In most practical applications, Q=2, 3, or 4 is used to provide computationally efficient results.

2.4. Analysis of bias $E\{\Delta\omega\}$ *and variance* $\mathrm{var}\{\Delta\omega\}$

The question that arises when dealing with the STFT based distributions is: what would be the optimal size of the two-dimensional window function used in the STFT calculation? Namely, it is important to analyze how the window size influences the representation and resolution of signal components or in other words what is the impact on bias. Furthermore, how does it influence the noise variance, and finally how is it possible to avoid the presence of cross-terms? Hence, this subsection is devoted to the window influence on the quality SSF representation.

The bias and the variance are related to the frequency ω: $E\{\Delta\omega\}$ and $\mathrm{var}\{\Delta\omega\}$. Since, we have two frequency coordinates $\vec{\omega}=(\omega_1,\omega_1)$, $\omega_1=2\pi k_x$, $\omega_2=2\pi k_y$, we will actually analyse bias and variance along ω_i, i=1,2. Let us observe a 2D noisy signal model:

$f(x,y)=s(x,y)+\nu(x,y)=A(x,y)e^{j\varphi(x,y)}+\nu(x,y)$, where $\nu(x,y)$ is noise. Furthermore, let C be the amplitude estimate for a considered signal harmonic, while $\vec{\omega}=(\omega_1,\omega_2)$ is the instantaneous frequency estimate. The estimation error can be written as follows:

$$\begin{aligned} e_{n_1,n_2} &= f(x+n_1T,y+n_2T)-Ce^{j(\omega_1 n_1 T+\omega_2 n_2 T)}= \\ &=\nu(x+n_1T,y+n_2T)+A(x,y)e^{j\varphi(x+n_1T,y+n_2T)}-Ce^{j(\omega_1 n_1 T+\omega_2 n_2 T)} \end{aligned} \tag{16}$$

where T is a sampling interval, $n_1,n_2\in[-N/2, N/2]$. By applying Taylor series expansion to the phase $\varphi(x+n_1T,y+n_2T)$ we have:

$$\varphi(x+n_1T,y+n_2T)=\varphi(x,y)+\varphi'(x,y)n_1Tn_2T+\delta\varphi(x+n_1T,y+n_2T)$$

where $\delta\varphi$ represents the terms producing the bias. If $\nu(x,y)=0$ and $\delta\varphi=0$, then by solving the minimization problem similar as in (2):

$$\begin{aligned} \vec{\omega}=(\omega_1,\omega_2)&=\arg\min_{\omega_1,\omega_2} J(x,y,\omega_1,\omega_2,C), \\ C&=\arg\min_{C} J(x,y,\omega_1,\omega_2,C) \end{aligned} \tag{17}$$

with the penalty function:

$$J(x,y,\omega_1,\omega_2,C)=\sum_{n_1}\sum_{n_2} w_h(n_1T,n_2T)(F(e_{1,n_1,n_2})+F(e_{2,n_1,n_2}))$$

we obtain $\vec{\omega}$ and C as the estimates of $\varphi'(x,y)$ and $A(x,y)$, respectively. Here, $w_h(n_1T,n_2T)=T/hw(n_1T/h,n_2T/h)$ is a window function, w is a real valued symmetric window, h is the window width (the STFT realization with constant h is considered), while $e_{1,n_1,n_2}=\mathrm{Re}\{e_{n_1,n_2}\}$, $e_{2,n_1,n_2}=\mathrm{Im}\{e_{n_1,n_2}\}$. However, when $\nu(x,y)\neq 0$ and $\delta\varphi\neq 0$, the bias and random errors appear in estimates. In the sequel, we focus on the analysis of bias and variance of $\vec{\omega}$. The necessary minimum condition can be given by:

$$\frac{\partial J}{\partial \omega_i^*}=\sum_{n_1}\sum_{n_2} w_h(n_1T,n_2T)\left(F^{(1)}(e_{1,n_1,n_2})\frac{\partial e_{1,n_1,n_2}}{\partial \omega_i^*}+F^{(1)}(e_{2,n_1,n_2})\frac{\partial e_{2,n_1,n_2}}{\partial \omega_i^*}\right). \tag{18}$$

For the bias estimation, without loss of generality, we may use: $\vec{\omega}=\varphi'(x,y),\ C=A(x,y)$. By applying the linearization with respect to small bias and small variance, the approximate expression for the bias is obtained in the form:

$$E\{\Delta\omega_i\}=\frac{\sum_{n_1}\sum_{n_2} w_h(n_1T,n_2T)n_iT\,\delta\varphi(x+n_1T,y+n_2T)}{\sum_{n_1}\sum_{n_2} w_h(n_1T,n_2T)\left(n_iT\right)^2}, \tag{19}$$

where the terms producing the bias are given by[1]:

$$\delta\varphi=\sum_{i=2}^{\infty}\frac{(\vec{n}T\nabla)^i\varphi(x,y)}{i!}\approx\frac{(\vec{n}T\nabla)^3\varphi(x,y)}{3!}. \tag{20}$$

Assuming that the separable window is used: $w_h(n_1T,n_2T)=w(n_1T/h)w(n_2T/h)$, we have:

$$E\{\Delta\omega_1\}_{i=1}=\frac{\sum_{n_1} w_h(n_1T)\left(n_1T\right)^4}{6\sum_{n_2} w_h(n_1T)\left(n_1T\right)^2}\cdot\frac{d\varphi^{(3)}(x,y)}{dx^3}+\frac{\sum_{n_2} w_h(n_2T)\left(n_2T\right)^2}{2}\cdot\frac{d\varphi^{(3)}(x,y)}{dxdy^2}$$, or in the integral form ($h/T\to\infty$):

$$E\{\Delta\omega_1\}=h^2\left(\frac{I(1,4)}{6I(1,2)}\frac{d\varphi^{(3)}(x,y)}{dx^3}+\frac{I(1,2)}{2}\frac{d\varphi^{(3)}(x,y)}{dxdy^2}\right), \tag{21}$$

$$I(1,4)=\int_{-1/2}^{1/2} w(t)t^4dt,\quad I(1,2)=\int_{-1/2}^{1/2} w(t)t^2dt.$$

Due to the window symmetry, the second phase derivative diminishes from the bias (the integral of an odd function over a symmetric interval is zero). The variance is given in the form:

[1]The expanded form can be written as: $\delta\varphi=\frac{(n_1T)^3}{6}\frac{d\varphi^{(3)}(x,y)}{dx^3}+3\frac{(n_1T)^2n_2T}{6}\frac{d\varphi^{(3)}(x,y)}{dx^2dy}+3\frac{n_1T(n_2T)^2}{6}\frac{d\varphi^{(3)}(x,y)}{dxdy^2}+\frac{(n_2T)^3}{6}\frac{d\varphi^{(3)}(x,y)}{dy^3}$.

$$\mathrm{var}\{\Delta\omega_1\}=\frac{\overline{\left(F^{(1)}\right)^2}}{\left(\left(\overline{F^{(2)}}\right)\right)^2}\frac{T^2}{|A|^2 h^4}\frac{I(2,2)}{\left(I(1,2)\right)^2}\cdot\frac{Iw(2)}{\left(Iw(1)\right)^2}, \tag{22}$$

$$I(2,2)=\int_{-1/2}^{1/2} w(t)^2 t^2 dt, \quad Iw(i)=\int_{-1/2}^{1/2} w^i(t)dt, \quad \overline{\left(F^{(1)}\right)^2}=\int\left(F^{(1)}(\nu)\right)^2 dG(\nu), \overline{\left(F^{(2)}\right)}=\int F^{(2)}(\nu)dG(\nu)$$

where G is the distribution of noise.

A very similar expression is obtained for the Wigner distribution and the S-method. We can observe that the bias decreases as the window width decreases, while the variance increases. Obviously, there is a bias-variance trade-off and the window width influences the results. Additionally, the concentration achieved by the distribution has an important impact, as well [11],[16]. For instance, for signals with fast varying periodical structures (2D chirps, interferograms, etc), the S-method provides highly concentrated signal components. By choosing small Q (e.g. Q=2) in (15), it will be less affected by noise than both the spectrogram and the Wigner distribution. For the calculation of the STFT (within the S-method), we can use a wide 2D window (e.g.,1/4 of each signal dimension), which will significantly decrease variance, while the bias is zero (for 2D chirps) or it is not influenced due to high concentration. For signals that are not periodical in the strict sense (i.e. irregularly periodical, such as textures), the narrow window (e.g., 1/10 of each signal dimension) should be used to provide periodicity within the window. Since the components within the narrow window are mostly linear, the spectrogram can be used. In this case, the S-method will not improve results noticeably, due to the dominant influence of narrow window. The influence of the window width has been examined experimentally later in Section 4 (Example 3).

3. L-ESTIMATE SPACE/SPATIAL-FREQUENCY BASED FILTERING

The stationary (space-invariant) filtering can be used in the case when signal and noise do not overlap in space and frequency domain. Otherwise, the nonstationary space-varying filtering should be used [16]. Namely, the signal and the noise can be separated within the joint SSF domain, which is a basis for an efficient SSF filtering procedure. The non-stationary space-varying filtering is realized by combining STFT with the support function L_H, [16]. The corresponding support function should be defined by using the L-estimate SSF distribution. For the noisy 2D signal $f(x,y)=s(x,y)+\nu(x,y)$, the pseudo form of the space-varying filtering is given by:

$$(Hf)(x,y)=\int_u\int_v h(x+\frac{u}{2},x-\frac{u}{2},y+\frac{v}{2},y-\frac{v}{2})\,f(x+u,y+v)dudv \tag{23}$$

where h is the impulse response of the space-varying two-dimensional filter. Space-varying transfer function in the Wigner distribution framework has been defined as Weyl symbol mapping of the impulse response into the space-spatial-frequency plane [16]:

$$L_H(x,y,k_x,k_y)=\int_{-\infty}^{\infty}\int_{-\infty}^{\infty} h(x,y,u,v)e^{-j\omega_x u-j\omega_y v}dudv. \tag{24}$$

Where $h(x,y,u,v)=h(x+u/2,x-u/2,y+v/2,y-v/2)$. By using the Moyal's formula for the inner product of signals and their Wigner distributions: $[WD_s(x,y),WD_z(x,y)]=|s(x,y)z(x,y)|^2$, the following ideal property should hold:

$$\begin{aligned}[(Hs)(x,y),s(x,y)]&=\int_{-\infty}^{\infty}\int_{-\infty}^{\infty}|s(x,y)|^2\,dxdy=\\ &=[1,WDs(x,y,k_x,k_y)]=[L_H(x,y,k_x,k_y),WDs(x,y,k_x,k_y)].\end{aligned} \tag{25}$$

Here, WD_s represents the mean of the Wigner distributions for different realizations of the signal and noise. However, we usually have to use the approximated Wigner distribution in practice, from a single noisy observation (as accurate as possible). Note that the S-method can be used in the case of multicomponent signals. By using the Parseval's theorem, the filtering relation (23) can be written as follows (discrete form is considered, since it is suitable for practical realizations):

$$y(x,y)=\sum_{k_x}\sum_{k_y}L_H(x,y,k_x,k_y)STFT_L(x,y,k_x,k_y), \tag{26}$$

where,

$$\begin{aligned}STFT_L(t,\omega)&=\sum_{u=-N/2}^{N/2-1}\sum_{v=-N/2}^{N/2-1}f(x+u,y+v)e^{-j\omega_x x}e^{-j\omega_y y}\\ &=\sum_{u=-N/2}^{N/2-1}\sum_{v=-N/2}^{N/2-1}sort\left\{f(x+u,y+v)e^{-j\omega_x x}e^{-j\omega_y y}\right\}\\ &\approx\sum_{p=0}^{N-1}\sum_{q=0}^{N-1}a_p a_q\left\{r_{p,q}(x,y,k_x,k_y)+ji_{p,q}(x,y,k_x,k_y)\right\}\end{aligned} \tag{27}$$

is an appropriate approximation of the STFT in the presence of heavy-tailed or mixed heavy-tailed and Gaussian noise. Note that due to α-trimming, the $STFT_L$ by itself provides filtering of strong peaks, even without applying the support function L_H. However, a significant amount of noise will be still present in the image. Hence, the $STFT_L$ provides an intermediate result, which is further processed and improved by using L_H, made as a binary map that identifies

components above a certain threshold. Hence, in order to define a support function, we consider the support region D defined as:

$$D=\left\{(x,y,k_x,k_y):\left|SSFD_L(x,y,k_x,k_y)\right|>\xi\right\}, \tag{28}$$

where ξ represents the energy floor, *SSFD* denotes a space/spatial-frequency distribution, while L indicates the L-estimate form (the L-estimate spectrogram or the L-estimate S-method). Therefore, D contains positions of relevant signal components within the $SSFD_L$. The energy floor is defined as a portion of the maximal value of the $SSFD_L$:

$$\xi=\lambda \max_{k_x,k_y}\{SSFD_L(x,y,k_x,k_y)\}. \tag{29}$$

Finally, the support function of the nonstationary space-varying filter can be defined in the form:

$$L_H(x,y,k_x,k_y)=\begin{cases}1 & \text{for} \quad (x,y,k_x,k_y)\in D\\ 0 & \text{for} \quad (x,y,k_x,k_y)\notin D\end{cases}. \tag{30}$$

Note that the space-varying filter performance will depend on the $SSFD_L$. It will be shown in the experiments that the optimal results are achieved by using the L-estimate S-method given by (15) ($SSFD_L=SM_L$) or the L-estimate spectrogram ($SSFD_L=SPEC_L$) given by (14).

The proposed robust space-varying filtering of images can be observed as a three-component filter form. The first part is based on the α-trimmed approach which is adapted to specific SSF components and removes noisy peaks. The second part is based on the mean filter in the SSF domain (for Gaussian white noise). The third part performs additional filtering by identifying specific and dominant signal components in the SSF domain by support function L_H and thresholding.

4. EXPERIMENTAL RESULTS

***Example1*:** The proposed approach for the robust SSF based filtering is tested on the analytical image given by:

$$s(x,y)=e^{j(-104\pi(x^2+x+y^2)}+e^{j(-104\pi(x^2+y+y^2)},$$

where $[0.1\le x\le 0.45]$, $[0.1\le y\le 0.45]$. Note that the considered signal has a form of interferogram image that appears in the optics [34]. The resolution of the considered sampled signal is 128x128 points. The noise is given by: $v(x,y)=0.5v_1^3(x,y)+0.5jv_2^3(x,y)$, where v_1 and v_2 are mutually independent Gaussian white noises (zero mean, variance 0.6). The SNR is -2.5 dB. The kurtosis is calculated as a measure of noise impulsiveness and the obtained value is 13 (for Gaussian white noise the value of kurtosis is 3).

The performance of the SSF representations, both the standard and the L-estimate forms, are analysed. The window size is 64×64. The energy floor ξ is calculated according to (29) with λ=0.2 (the value of λ is chosen experimentally using a large number of trials). The S-method is calculated by using Q=2. The L-estimate forms are calculated by using α=3/8, to provide good trade-off between noise reduction and distribution concentration. The components of the standard spectrogram selected by the support function L_H, are illustrated in Fig 1.a (for point (0.35,0.13)). Also, the S-method and its components, identified by the corresponding support function, are shown in Fig 1.b. Note that the standard forms are quite affected by the noise, and the corresponding space-varying filtering [16] cannot suppress the noise.

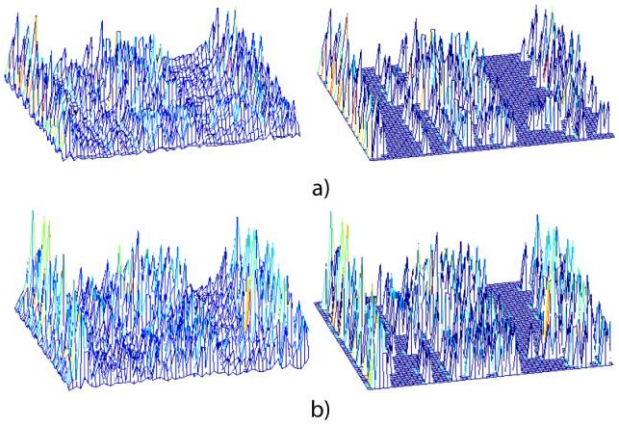

Fig 1. Standard distribution forms: a) spectrogram (left) and its components selected by the support function (right), b) S-method (left) and its components selected by the support function (right)

The L-estimate spectrogram and the L-estimate S-method are shown in Fig 2, for the same point. Note that the robust distributions significantly reduce the noise in comparison with the standard ones. Especially, the L-estimate S-method provides highly concentrated components (Fig 2.b, left). Thus, the support function can easily identify signal components while removing the noise influence (Fig 2.b, right). Next we consider the filtering results. The original noise-free signal $s(x,y)$ is shown in Fig 3.a, while the noisy signal is shown in Fig 3.b. For the comparison with the proposed approach, various existing filtering procedures are considered: spatial domain filtering based on the 3×3 median filter (Figs 3.c), filter form proposed in [3] (Figs 3.d). In both cases, the filters produce poor results. Furthermore, the frequency domain procedures are tested: a low-pass filter with cut-off frequency $f=f_{max}/2$ to reduce Gaussian noise, and a band-stop filter with boundaries $f_h=3f_{max}/4$ and $f_l=f_{max}/4$ to reduce impulse noise [35]. The results are shown in Fig 3.e and Fig 3.f, respectively. The space-varying filtering procedures [16] based on the standard spectrogram (Fig 3.g) and the standard S-method (Fig 3.h) are also considered, but they are only suitable for Gaussian noise. Finally, the proposed approach is performed by using the L-estimate spectrogram (Fig 3.i) and the L-estimate S-method (Fig 3.j). Note that the best quality

is achieved by using the L-estimate S-method. The SNR after the proposed filtering approach has increased to 13 dB from the starting -2.5 dB. The achieved SNR values for other considered filters are given in Table 1.

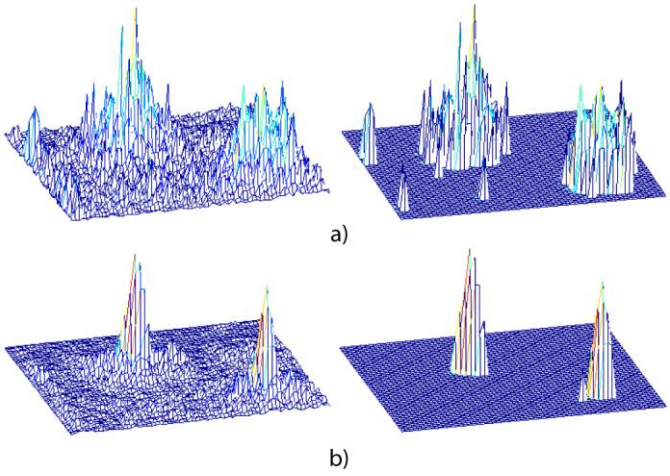

Fig 2. L-estimate distribution forms: a) L-estimate spectrogram (left) and its components identified by the support function (right), b) L-estimate S-method (left) and its components identified by the support function (right)

TABLE 1. SNR VALUES FOR DIFFERENT FILTERS

Filter type	**SNR (dB)**
median filter	-0.9
peak-and-valley filter	5.1
low pass filter	0.66
band stop filter	0.06
space-varying filter based on the standard spectrogram	2
space-varying filter based on the standard S-method	6.1
space-varying filter based on the L-estimate spectrogram	5.8
space-varying filter based on the L-estimate S-method	13

Example 2: In this example, the proposed approach is tested for texture images (e.g. Brodatz textures), images with fast varying non-stationary periodical structures and satellite image. The original test images are subsampled by factor 2 or 4 in order to provide variations within a few pixels. The images are then corrupted by a heavy-tailed noise (Table 2) and mixed noise (Table 3). Non-noisy images are given in the 1st row (Tables 2 and 3), while the noisy images are given in the 2nd row. The images filtered using the median filter 3×3 and 5×5 are shown in the 3rd and 4th row in Table 2, respectively. Furthermore, in Table 2 we include results obtained for total variation[2] (TV) filtering [7] in the 5th row, the filter based on variational approach to remove outliers and impulse noise [9] (6th row, the parameter β=0.2 is used).

[2] parameters: *iter* - number of iterations, *dt* - time step, λ - fidelity term

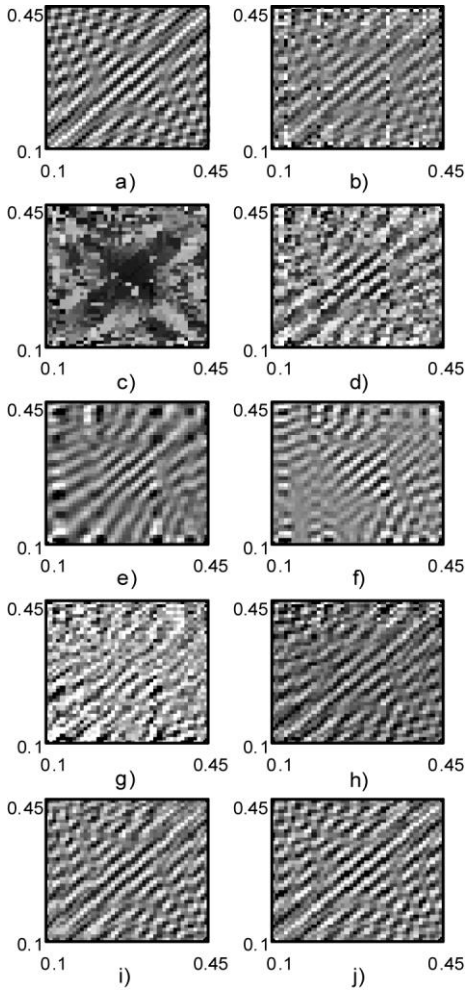

Fig 3: a) Original image, b) Noisy image; Images filtered by: c) median filter, d) peak-and-valley filter proposed in [3], e) low pass filter, f) band stop filter, g) space-varying filter based on the standard spectrogram, h) space-varying filter based on the standard S-method, i) space-varying filter based on the L-estimate spectrogram, j) space-varying filter based on the L-estimate S-method

The results obtained by using the space-varying approach [16] are given in the 7^{th} row. Finally, the results obtained by using the proposed robust non-stationary filter are given in the 8^{th} row. It can be observed that in all considered cases the proposed approach provides better results than the other considered filters and enhances a visual quality of images. Note that the TV and variational approach [9] remove noisy peaks, but it is difficult to deal with noisy patches that exist in this case, and a certain blurring is introduced lowering the PSNR. Similar performance of the proposed approach is achieved for mixed Gaussian and heavy-tailed noise (the results are shown in Table 3). For the comparison purpose, we have included the results obtained by using TV and detail-preserving regularization method [10] for the mixed noise. This method has two parameters c and λ. The parameter controlling smoothing level is λ=0.05 (different values of λ are tested and 0.05 is chosen as an optimal value). Higher λ may additionally reduce the noise, but introduces more blurring. The parameter c depends on the degree at which the discontinuities in the image should be retained (c=6 is used as in [10]). Here, it is important to emphasize that the noise is spread over all pixels, i.e., entire pixels neighbourhoods are corrupted

by noise, causing that the considered reconstruction methods cannot work properly. From Table 3, we might observe that again the proposed filtering procedure provides the highest quality of images due to the advantages of L-estimation approach.

The previous experiments show that the proposed method is highly efficient for signals with specific frequency components. These signals appear in numerous real-life applications such as in optics, machine vision, automated inspection problems, surface inspection, medical applications, defect detection, etc. Their common characteristic is based on a set of frequency components that are more pronounced than the others. The proposed approach preserves important frequency components, which are crucial for texture quality. In the case of natural images (Lena or Baboon), instead of textures, we have non-uniformly distributed surfaces. Hence, we cannot identify the dominant frequency peaks, since the components are spread over the SSF plane in the same way as the noise. This is in accordance with the principles of the SSF analysis, which are hardly applicable in such an environment.

TABLE 2. FILTERING RESULTS FOR SOME OF THE TEST IMAGES IN THE CASE OF IMPULSE NOISE

	1.	2.	3.	4.	5.
Original image	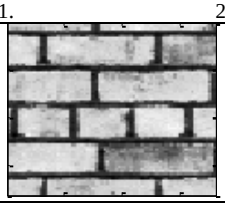	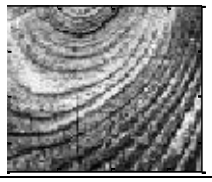		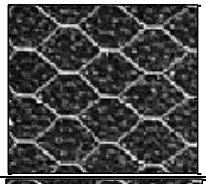	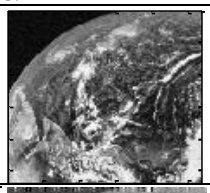
Noisy Image (imp noise)	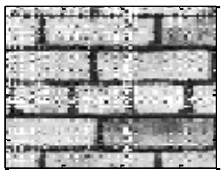	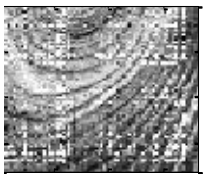		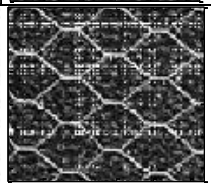	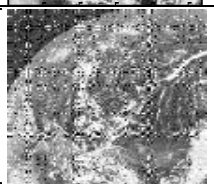
	PSNR=11 dB	PSNR=8.16 dB	PSNR=11.2 dB	PSNR=9.4 dB	PSNR=9.8 dB
Median 3x3	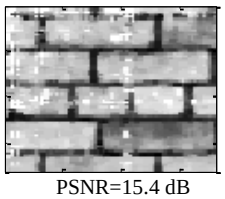	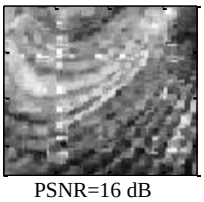	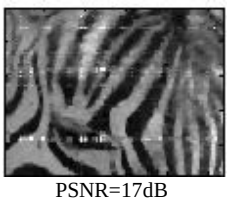	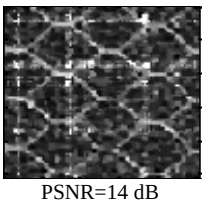	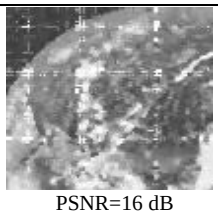
	PSNR=15.4 dB	PSNR=16 dB	PSNR=17dB	PSNR=14 dB	PSNR=16 dB
Median 5x5	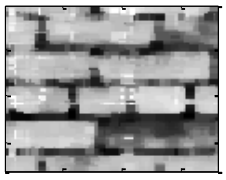	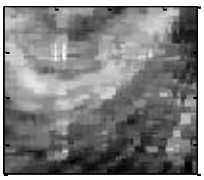		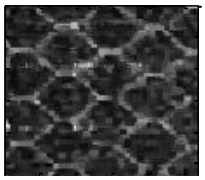	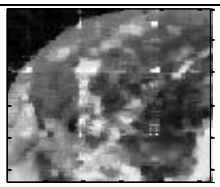
	PSNR=16 dB	PSNR=14 dB	PSNR=18.8 dB	PSNR=14.5 dB	PSNR=17.4dB
TV		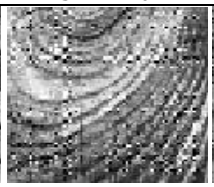		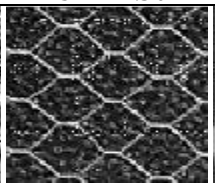	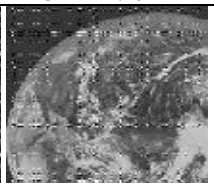
	iter=40, dt=0.5, λ=1 PSNR=8.4 dB	iter=50, dt=0.2, λ=2 PSNR=7.6 dB	iter=50, dt=0.5, λ=1 PSNR=11.6 dB	iter=50,dt=0.3,λ=0.8 PSNR=14.6 dB	iter=50,dt=0.4, λ=1 PSNR=14 dB
Variation. approach				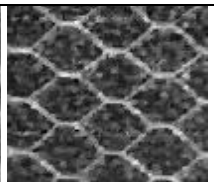	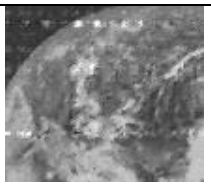
	PSNR=15.2 dB	PSNR=15dB	PSNR=17.2 dB	PSNR=15.3 dB	PSNR=19 dB
Standard SSF filtering	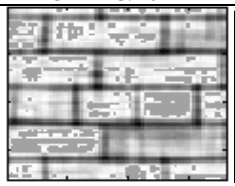	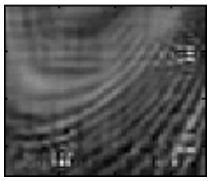	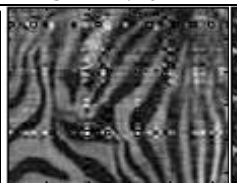	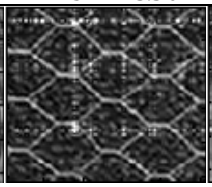	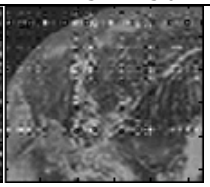
	PSNR=16 dB	PSNR=14 dB	PSNR=18 dB	PSNR=16 dB	PSNR=17 dB
Proposed filtering	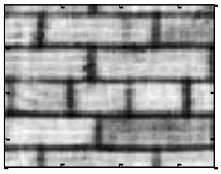	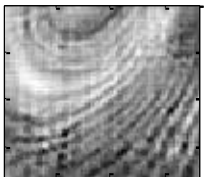	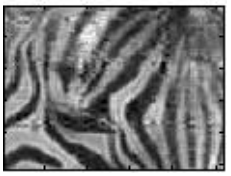	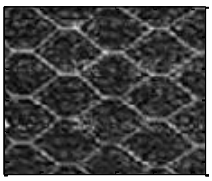	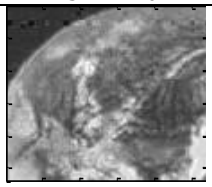
	PSNR=21dB	PSNR=18.3 dB	PSNR=21dB	PSNR=19.3 dB	PSNR=19.1 dB

TABLE 3. FILTERING RESULTS FOR SOME OF THE TEST IMAGES IN THE CASE OF MIXED NOISE

	1.	2.	3.	4.	5.
Original image					
Noisy Image (mixed noise)	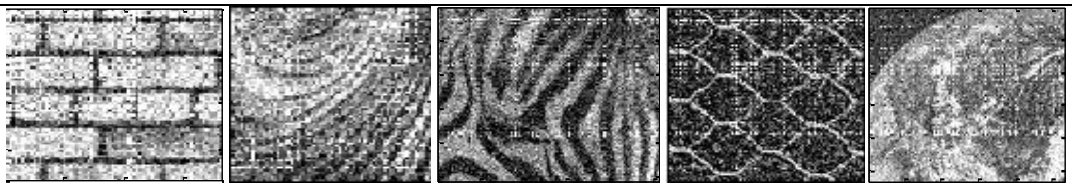	PSNR=6.8dB	PSNR=8dB	PSNR=11 dB	PSNR=9.6 dB	PSNR=9 dB
TV	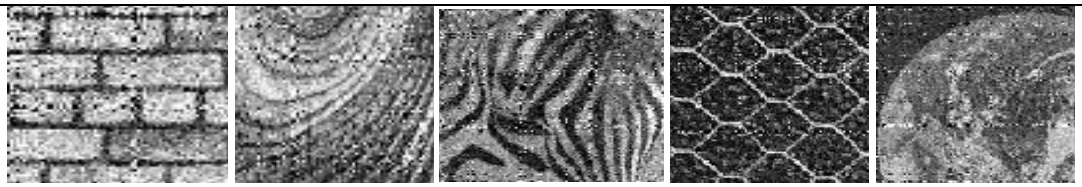	iter=40, dt=0.5, λ=1 PSNR=7.6 dB	iter=50, dt=0.2, λ=2 PSNR=7 dB	iter=50, dt=0.5, λ=1 PSNR=11.5 dB	iter=50,dt=0.3,λ=0.8 PSNR=14.5 dB	iter=50,dt=0.4, λ=1 PSNR=12 dB
Detail-Presser. regulariz	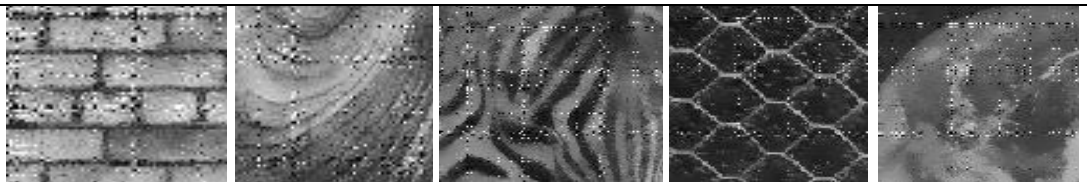	λ=0.05, c=6 PSNR=8.5 dB	λ=0.05, c=6 PSNR=9 dB	λ=0.05, c=6 PSNR=12 dB	λ=0.05, c=6 PSNR=15 dB	λ=0.05, c=6 PSNR=12.5 dB
Proposed filtering	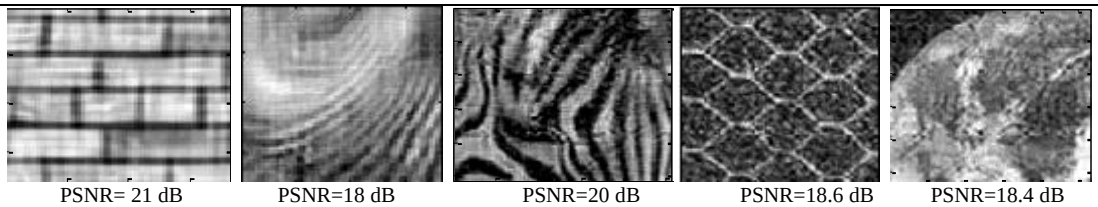	PSNR= 21 dB	PSNR=18 dB	PSNR=20 dB	PSNR=18.6 dB	PSNR=18.4 dB

Example 3: The influence of window width is considered in this last example. Two cases have been observed: 1) 2D chirp signals as in Example 1; 2) sample texture image from Example 2. As it is discussed in Section 3, we aim to demonstrate that in the case of interferograms and chirp-like signals with fast varying structures, a wide window should be used in $STFT_L$, since it will minimize the variance, while the bias is approximately zero. The texture-like images should be treated with a narrow window, which will linearize the spectrum and make the spectrogram suitable for analysis and filtering. The filtering results for 2D chirp signal and different window widths: w=8, w=16, w=32 and w=64 samples, are given in Table 4. Observe that the results are improved by increasing w. An optimal choice is w=64. A wider window (e.g., 128 samples) achieves the same visual quality and the same SNR improvement. The texture images are

considered in Table 5. The results of the proposed filtering are tested for: w=64, w=32, w=16 and w=8 samples. As expected, the best results are obtained for narrow window w=8.

TABLE 4. 2D CHIRP: INFLUENCE OF THE WINDOW WIDTH

2D chirp, SNR_0=-2.5dB				
	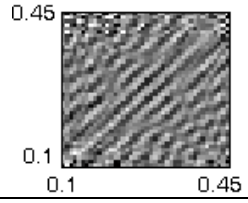	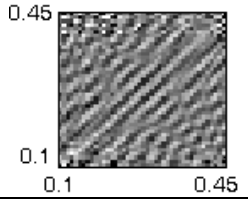	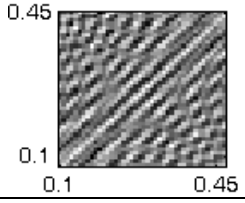	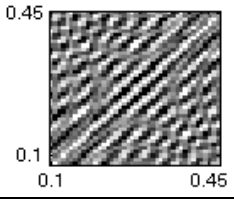
w	8	16	32	64
SNR	1.12dB	7.5dB	9.1dB	13dB

TABLE 5. SAMPLE TEXTURE IMAGE: INFLUENCE OF THE WINDOW WIDTH

Texture Image, $PSNR_0$=9dB				
	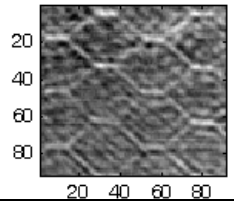	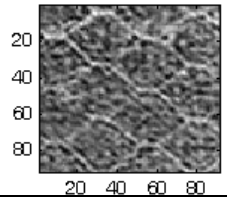	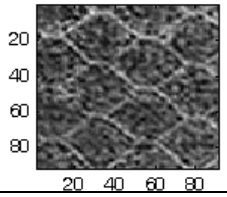	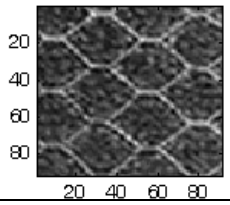
w	64	32	16	8
SNR	13dB	14dB	17dB	19dB

5. CONCLUSION

In this paper, we consider denoising of non-stationary 2D signals corrupted by a heavy tailed or mixed heavy-tailed and Gaussian noise. The considered signals/images are characterized by the specific frequency content, which produces fast-varying details and structures in the spatial domain. Hence, to provide their appropriate analysis, the 2D L-estimate space/spatial-frequency distributions are proposed. Furthermore, in order to deal with strong heavy-tailed and mixed heavy-tailed and Gaussian noise, the L-estimate form of space-varying filtering is defined. The experiments have shown that the images filtered by the non-stationary space-varying L-estimate approach retain good visual quality and readability even

for a high amount of noise. In these cases, the proposed filter form outperforms commonly used stationary filters, edge and detail-regularization approaches, variational approaches, etc. Note that the L-estimate filter form in the space/spatial-frequency domain introduces slight image blurring effects. Hence, the future research may be dedicated to an image sharpening and deblurring procedure that should be applied after the L-estimate filtering approach.

ACKNOWLEDGEMENT

The authors would like to thank their colleagues Dr. Nikola Žarić and Branka Jokanović for useful discussions and help in some parts of the examples.

REFERENCES

[1] B. Barkat and LJ. Stanković, Analysis of Polynomial Signals Corrupted by Heavy-Tailed Noise, Signal Processing, 84(1), 2004, pp. 69-75.

[2] A. B. Hamza and H. Krim, Image Denoising: A Nonlinear Robust Statistical Approach, IEEE Transactions on Signal Processing, 49(12), 2001, pp. 3045-3054.

[3] N. Alajlan, M. Kamel, E. Jermigam, Detail preserving impulsive noise removal, Signal Processing: Image Communication, 19(10), 2004, pp. 993-1003.

[4] M. Juneja, R. Mohana, An Improved Adaptive Median Filtering Method for Impulse Noise Detection, Int. Journal of Recent Trends in Engineering, 1(1), 2009, pp. 274-278.

[5] G. Wang, D. Li, W. Pan and Z. Zang, Modified switching median filter for impulse noise removal, Signal Processing, 90(12), 2010, pp. 3213-3218.

[6] V. V. Lukin, D. V. Fevralev, N. N. Ponomarenko, S. K. Abramov, O. B. Pogrebnyak, K. O. Egiazarian, J. T. Astola, Discrete cosine transform–based local adaptive filtering of images corrupted by nonstationary noise, Journal of Electronic Imaging, 19(2), 2010, 023007.

[7] L. Rudin, S. Osher and E. Fatemi, Nonlinear Total Variation Based Noise Removal Algorithms, Physica D, 60 (1992), pp. 259–268.

[8] L.A. Vesse and S. J. Osher, Modeling Textures with Total Variation Minimization and Oscillating Patterns in Image Processing, Journal of Scientific Computing, 19(1-3), 2003, pp.553-572.

[9] M. Nikolova, A variational approach to remove outliers and impulse noise, Journal Math. Imaging Vision, 201–2, 99–120, 2004.

[10] X. Zeng and L. Yang, Mixed impulse and Gaussian noise removal using detail-preserving regularization, Optical Engineering, 49, 2010, 097002.

[11] S. Stanković, LJ. Stanković, Z. Uskoković, On the local Frequency, Group Shift and Cross Terms in Some Multidimensional Time-Frequency Distributions; A Method for Multidimensional Time-Frequency Analysis, IEEE Transactions on Signal Proc*essing*, 43(7), 1995, pp. 1719 – 1724.

[12] LJ. Stankovic, S. Stankovic, Wigner distribution of noisy signals, IEEE Transactions on Signal Processing, 41(2), 1993, pp.956-960.

[13] Y. M. Zhu, R. Goutte, M. Amiel, On the use of a two-dimensional Wigner-Ville distribution for texture segmentation, Signal Processing, 30(3), 1993, pp. 205-222.

[14] G. Cristobal, J. Bescos, J. Santamaria, Image Analysis through the Wigner distribution function, Appl. Optics, 28(2), 1989, pp. 262-271.

[15] A. Beghdadi, R. Iordache, Image Quality Assessment Using the Joint Spatial/Spatial-Frequency Representation, EURASIP Journal on Applied Signal Proc, 2006, Article ID 80537, pp. 1–8.

[16] LJ. Stanković, S. Stanković, I. Djurović, Space/Spatial-Frequency Based Filtering, IEEE Transactions on Signal Processing, 48(8), 2000, pp. 2343-2352.

[17] I. Djurović, LJ. Stanković, J. F. Böhme, Robust L-estimation based forms of signal transforms and time-frequency representations, IEEE Transactions Signal Processing, 51(7), 2003, pp.1753-1761.

[18] I. Djurović, LJ. Stanković, Robust Wigner Distribution with Application to the Instantaneous Frequency Estimation, IEEE Transactions on Signal Processing, 4(12), 2001, pp. 2985 – 2993

[19] I. Orović, N. Žarić, S. Stanković, Robust Space/Spatial-Frequency Based Filtering of Images in the Presence of Heavy Tailed Noise, 20th Int. Conf. on Computer Graphics and Vision, Sept. 2010.

[20] P.J. Huber, Robust Statistics, John Wiley&Sons Inc., 1981.

[21] B.T. Poljak, J.Z. Tsypkin, Robust identification, *Automatika*, 16, 1980, pp. 53-63.

[22] I. Pitas, A.N. Venetsanopoulos: Nonlinear digital filters: Principles and applications, Kluwer, 1990.

[23] I. Pitas, A.N. Venetsanopoulos, Order Statistics in Digital Image Processing, Proc. IEEE, 80, 1992, pp. 1893-1992.

[24] M. Pappas, I. Pitas: Multichannel distance filter, IEEE Transactions on Signal Processing, 47(12), 1999, pp. 3412-3416

[25] A. Ben Hamza, H. Krim: Image denoising: A nonlinear robust statistical approach, IEEE Transactions on Signal Processing, 49(12), 2001, pp. 3045-3054

[26] H. Krim, I.C. Schick: Minimax description length for signal denoising and optimized representation, IEEE Transactions on Information Theory, 45(3), 1999, pp. 898-908

[27] D. Pastor, Robust Estimation of Noise Standard Deviation in Presence of Signals With Unknown Distributions and Occurrences, IEEE Transactions on Signal Processing, 60(4), 2012, pp. 1545-1555.

[28] B. Boashash, Time Frequency Signal Analysis and Processing: A Comprehensive Reference, Elsevier, 2003.

[29] E. Otez and R.J.P. Figueiredo, Adaptive Alpha-Trimmed Mean Filters Under Deviations From Assumed Noise Model, IEEE Transactions on Image Processing, 13(5), 2004, pp. 627-639

[30] N. Zarić, N. Lekić, S. Stanković, An Implementation of the L-estimate Distributions for Analysis of Signals in Heavy-Tailed Noise, IEEE Trans. on Circuits and Systems II, 58(7), 2011, pp.427-431.

[31] LJ. Stanković, A method for Time-Frequency Signal Analysis, IEEE Transactions on Signal Processing, 42(1), 1994, pp. 225 – 229.

[32] T. Thayaparan, LJ. Stanković, C. Wernik, and M. Daković: Real-time motion compensation, image formation and image enhancement of moving targets in ISAR and SAR using S-method based approach, IET Signal Processing, 2(3), 2008, pp. 247-264.

[33] S. Stanković, I. Orović, and A. Krylov, Video Frames Reconstruction Based on Time-Frequency Analysis and Hermite Projection Method, EURASIP Journal on Advances in Signal Processing, 2010, Article ID 970105, 11 pages.

[34] M. Servin, M. Cywiak, D. Malacara-Hernandez, J. C. Estrada, J. A. Quiroga, Spatial carrier interferometry from M temporal phase shifted interferograms: Squeezing Interferometry, Optics Express, 16(13), 2008, pp. 9276-9283.

[35] R. C. González, R. E. Woods, Digital image processing, 3th Edition, Prentice Hall, 2007.